Microelectronic Engineering 20 (1993) 43–54
Elsevier

Simulation of growth in pyrolytic laser-CVD of microstructures—II. Two-dimensional approach

N. Arnold and D. Bäuerle
Angewandte Physik, Johannes-Kepler-Universität Linz, A-4040 Linz, Austria

Abstract. Pyrolytic laser-CVD of microstructures is simulated in a two-dimensional self-consistent numerical calculation. The model is applied to the deposition of spots and the direct writing of lines.

Keywords. Laser-induced deposition; Modelling

1. Introduction

In previous papers we have investigated different theoretical descriptions of pyrolytic laser-induced chemical vapor deposition (LCVD). In one type of approach the temperature rise induced by the absorbed laser light on the surface of the deposited material is assumed to be known and independent of the geometry of the deposit. The reaction flux is then calculated by considering different types of gas-phase transport as well as heterogeneous or/and homogeneous activation of the reaction. The main results achieved in these investigations are presented in [1–4]. This type of approach, however, does not even permit a semi-quantitative analysis of the experimental data. The reason is the strong dependence of the laser-induced temperature distribution on the geometry of the deposit. This has already been outlined in [5]. In a foregoing paper [6] we have accounted for this problem within the framework of a one-dimensional model. This model can be applied to laser direct writing. Here, the equation of growth was solved simultaneously with an analytic equation that approximates the laser-induced temperature distribution on the surface of the deposited stripe.

In the present paper, we present a two-dimensional self-consistent calculation of the equation of growth and the heat equation. Clearly, only numerical techniques can be employed in this case. As in [6], we assume a purely

Correspondence to: Prof. D. Bäuerle, Angewandte Physik, Johannes-Kepler-Universität Linz, A-4040 Linz, Austria.

heterogeneous reaction and ignore any gas-phase transport. Even with these assumptions, considerable computational efforts are required. Examples for the simulation of growth of spots and the direct writing of lines will be presented.

2. Model

The model employed in the calculations is schematically shown in Fig 1. The deposit is placed on a semi-infinite substrate; the respective thermal conductivities and temperatures are denoted by κ_D, T_D and κ_S, T_S. For the same reasons as in [6] we consider the case $\kappa^* = \kappa_D/\kappa_S \gg 1$. The origin of the coordinate system is fixed with the laser beam and indicated by a dot. In the

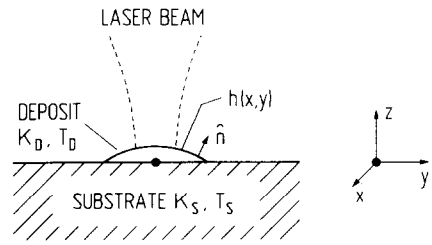

Fig. 1. Schematic picture of a two-dimensional model for the description of pyrolytic laser-CVD. The origin of the coordinate system is indicated by the dot. The surface of the deposit is described by $h(x, y)$. $\hat{n}$ is a unit vector normal to $h(x, y)$.

Nikita Arnold was born in 1965, Moscow, Russia. He graduated from Moscow Institute of Physics and Technology in 1987, and obtained his PhD in Physics in 1990. Since 1990 he is a research fellow in the Institute of General Physics, Russian Academy of Sciences, Moscow. In 1991/1992 he was a visiting scientist in the Institute of Applied Physics, Johannes-Kepler-University, Linz, Austria. His research interest is in the field of computer simulations of nonlinear phenomena in distributed systems. He has more than ten publications on this subject.

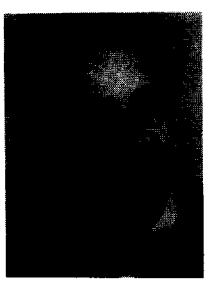

Dieter Bäuerle received his PhD from the University of Stuttgart. Since 1978 he is Professor for Applied Physics at the Johannes-Kepler-University in Linz, Austria. He worked for several years at Cornell University, Ithaca, at the Philips Research Lab in Aachen, and the Max-Planck-Institut for Solid State Research in Stuttgart. He has made contributions in many areas of solid-state physics, laser physics, and spectroscopy, including lattice dynamics, structural phase transitions, high-temperature superconductors, laser chemical processing, and in-situ spectroscopy in reactive systems. He has published over 140 papers, 14 patents, 7 books, and received several awards. He is a member of the Austrian Physical Society, German Physical Society and European Physical Society.

case of direct writing, scanning shall exclusively be performed in the x-direction with the velocity v_S. The shape of the deposit is described by an arbitrary function $h(x, y)$ with $0 < z < h(x, y)$.

2.1. *The heat equation*

The temperature distribution induced by the absorbed laser light can be calculated from the boundary-value problem

$$c_D \rho_D \frac{\partial T_D}{\partial t} - \nabla_3[\kappa_D(T_D)\nabla_3 T_D] = Q(x, y, z, t)\,, \tag{1}$$

$$\kappa_D(T_D) \frac{\partial T_D}{\partial z}\bigg|_{z=0} = J_{loss}(z = 0)\,,$$

$$-\kappa_D(T_D) \frac{\partial T_D}{\partial \hat{n}}\bigg|_{z=h} = J_{loss}(z = h)\,.$$

c_D is the specific heat and ρ_D the mass density of the deposit. The index 3 at the nabla operator stands for the three dimensions. Q is the source term, and J_{loss} describes the energy loss at surfaces $z = 0$ and $z = h$. The unit vector $\hat{n} = \boldsymbol{n}/|\boldsymbol{n}|$ is directed normally to the surface $z = h(x, y)$ so that $\boldsymbol{n} = \{-\partial h/\partial x, -\partial h/\partial y, 1\}$. In principle, the boundary-value problem (1), together with the corresponding equations for the substrate, and the equation of growth (Section 2.2), can directly be solved numerically. It is, however, more convenient to use some further approximations and transformations.

The integration of (1) within the region $0 \leqslant z \leqslant h$ yields

$$\int_0^h c_D \rho_D \frac{\partial T_D}{\partial t}\,\mathrm{d}z = \int_0^h \frac{\partial}{\partial z}\left(\kappa_D(T_D)\frac{\partial T_D}{\partial z}\right)\mathrm{d}z + \int_0^h \nabla_2[\kappa_D(T_D)\nabla_2 T_D]\,\mathrm{d}z + \int_0^h Q(x, y, z, t)\,\mathrm{d}z\,. \tag{2}$$

We now make the following assumptions: The deposit shall be flat, so that $\partial h/\partial x \ll 1$. Thus,

$$\frac{\partial T_D}{\partial \hat{n}} = \frac{\partial T_D}{\partial z} - \nabla_2 h \cdot \nabla_2 T_D\,. \tag{3}$$

Furthermore, we assume $T_D \equiv T_D(x, y, z, t) \approx T_D(x, y, 0, t)$ which holds if $h/[r_D \kappa^*] \ll 1$ (this follows from $\kappa_D\,\partial T_D/\partial z = \kappa_S\,\partial T_S/\partial z$ and $\partial T_S/\partial z \approx [T_S(z = 0) - T(\infty)]/r_D$). In this case we can expand T_D in a Taylor series and take into account only the first term

$$T_D(z) = T_D(z = 0) + O(z)\,. \tag{4}$$

With these approximations (2) can be written as

$$c_D \rho_D h \frac{\partial T_D}{\partial t} = \nabla_2[h\kappa_D(T_D)\nabla_2 T_D] + \int_0^h Q \, dz - J_{loss}(z = h) - J_{loss}(z = 0) . \quad (5)$$

Equation (5) is just the energy balance for a volume element of the deposit with a basal area $dx\,dy$ and a height $h(x, y)$. We now make some further simplifying assumptions:

(i) Growth shall be quasi-stationary. Thus, the time to reach thermal equilibrium is $\tau_T \ll [\partial(\ln h)/\partial t]^{-1}$. For the same reason, we ignore any changes in temperature distribution due to the scanning of the laser beam.

(ii) Heat losses to the gas phase shall be ignored, i.e. $J_{loss}(z = h) = 0$. At the interface $z = 0$ we set

$$J_{loss}(z = 0) = \kappa_S(T_S) \frac{\partial T_S}{\partial z}\bigg|_{z=0} . \quad (6)$$

(iii) We assume that the laser light is totally absorbed within the deposit, i.e.

$$\int_0^h Q \, dz = I_a(x, y) = AI(x, y) , \quad (7)$$

where A is the absorptivity. By introducing the linearized temperatures θ_D and θ_S via the Kirchoff transform, we obtain from (5)–(7)

$$\kappa_S(T(\infty)) \frac{\partial \theta_S}{\partial z}\bigg|_{z=0} = I_a(x, y) + \kappa_D(T(\infty))\nabla_2[h(x, y)\nabla_2 \theta_D] . \quad (8)$$

The second term on the right side originates from the "lateral spreading" of the surface temperature θ_D due to the deposit. Equation (8) can be considered as a modified boundary condition for calculating the (stationary) temperature distribution in the substrate. This is given by the Laplace equation

$$\nabla_3^2 \theta_S = 0 . \quad (9)$$

Using the Green's function technique, the solution can be written in the form

$$\theta_S = \frac{1}{2\pi} \int_{-\infty}^{+\infty} \int \frac{\partial \theta_S}{\partial z'}\bigg|_{z'=0}(x', y') \times [[x - x']^2 + [y - y']^2 + z^2]^{-1/2} \, dx' \, dy' . \quad (10)$$

For the surface $z = 0$ this becomes

$$\theta_S(\boldsymbol{r}) = \frac{1}{2\pi} \left\{ \frac{\partial \theta_S}{\partial z} * \frac{1}{|\boldsymbol{r}|} \right\}$$

where $\boldsymbol{r}$ is a two-dimensional radius vector within the xy-plane and $*$ denotes

the convolution integral

$$\{f * g\} \equiv \int_{-\infty}^{+\infty} \int f(r') \cdot g(r - r')\, \mathrm{d}x'\, \mathrm{d}y' .$$

Thus, (8) yields

$$\theta_S = \theta_S^0 + \frac{\kappa^*(T(\infty))}{2\pi} \left\{ \nabla_2 [h \nabla_2 \theta_D] * \frac{1}{|r|} \right\}, \tag{11}$$

where

$$\theta_S^0 = \frac{1}{2\pi \kappa_S(T(\infty))} \left\{ I_a * \frac{1}{|r|} \right\}$$

is the (linearized) temperature distribution without the deposit; θ_S^0 remains unchanged during the growth process as long as the absorptivity, A, stays constant. If A changes, (11) is still valid. In this case, however, the computational time will increase significantly. Clearly, at $z = 0$ the temperatures θ_S and θ_D are related via the condition

$$T_D(\theta_D) = T_S(\theta_S) \quad \text{at } z = 0 .$$

As a consequence we have

$$\theta_S = \theta_S(\theta_D) . \tag{12}$$

This dependence can be rather complicated (it is always monotonously increasing) and it is therefore convenient to draw a parametric plot in the (θ_S, θ_D)-plane. The dependence $\theta_S(\theta_D)$ is then fitted by a polynom of the form

$$\theta_S = \theta_D + \alpha \theta_D^2 + \cdots .$$

With this substitution, (11) becomes a nonlinear integro-differential equation for the determination of θ_D. In the absence of the deposit ($h = 0$), equation (11) describes the linearized temperature on the surface of the substrate. If $h \neq 0$, the second term in (11) is non-zero. The real temperature is obtained from the inverse Kirchhoff transform after solving (11). Thus

$$T(h(x, y)) = T_D(\theta_D) .$$

The advantage of solving (11) instead of the original boundary-value problem (1) is:

- It is two-dimensional, but describes the temperature distribution of a three-dimensional problem.
- No boundary conditions must be considered. They are included implicitly in θ_S and θ_D.

- Any temperature dependences in κ_D and κ_S can easily be taken into account.
- It is sufficient to confine the convolution integrals to the region where $h \neq 0$ and $I_a \neq 0$.

2.2. *Equation of growth*

In the coordinate system fixed with the beam the shape of the deposit can be described by

$$\frac{\partial h}{\partial t} = W(T_D) + v_S \frac{\partial h}{\partial x} . \tag{13}$$

The growth rate $W(T_D)$ follows an Arrhenius type law

$$W(T_D) = k_0 \exp\left(-\frac{\Delta E^*}{T_D}\right)\left[1 + \exp\left(\frac{T_{th} - T_D}{\delta T_{th}}\right)\right]^{-1} , \tag{14}$$

where k_0 is the usual pre-exponential factor in the Arrhenius law, and $\Delta E^* = \Delta E / k_B$ the apparent chemical activation energy in kelvin. The additional factor in (14) shall account for the threshold behavior of the deposition process, i.e. for the fact that deposition becomes significant only if T_D exceeds the threshold temperature, T_{th}. The width of this threshold, which describes the drop in deposition rate near T_{th}, is denoted by δT_{th}. The boundary and initial conditions for (13) are usually characterized by $h = 0$.

3. Numerical procedure

The numerical calculations of the temperature distribution—with stationary shape of the deposit—are performed by employing the following iteration procedure

$$\theta_D^{i+1} = \theta_D^i + c\left[\frac{2\pi}{\kappa^*(T(\infty))}\left[\theta_S^0 - \theta_S(\theta_D^i)\right] + \left\{\nabla_2\left[h\nabla_2\theta_D^i\right] * \frac{1}{|r|}\right\}\right] , \tag{15}$$

where i denotes the step of iteration. The last term was discretized by employing the finite difference technique. The coefficient $c > 0$ determines the convergence of the iteration procedure.

Equation (13) was solved by splitting the process of growth and advection (scanning). The growth of the deposit, which is determined by the first term in (13), was simulated by an implicit scheme with respect to the height, h, as a function of time, t. This scheme was solved using an iteration procedure with respect to h. After each step of iteration for the height h, the temperature distribution was recalculated from (15). Iteration was stopped when changes in subsequent h-iterations became sufficiently small. The time step for advection (second term in (13)) was chosen in the usual way for upwind schemes, $\tau = \Delta x / v_S$, and was much larger than the step for growth.

4. Simulation of growth

The model calculations shall now be applied to the deposition of spots and the direct writing of lines by pyrolytic laser-CVD. As practical examples we choose the deposition of W and Ni onto quartz (SiO_2) substrates. The substrates employed in the experiments were frequently coated with a thin film of sputtered W or amorphous Si (typically 700 to 1200 Å thick) [5, 7, 8]. Such a film permits a well-defined initiation of the deposition process [5]. Its influence on the temperature distribution has been ignored in the present calculations.

For convenience, we introduce normalized quantities and indicate them by an asterisk. h, x, y, v_S, and k_0 are normalized to the radius of a Gaussian laser beam, w_0. Correspondingly, all temperatures and activation energies are normalized to the temperature $T(\infty)$. The normalized intensity is $I_0^* = I_0 w_0 / [T(\infty) k_S(T(\infty))]$.

4.1. *Growth of spots*

Figure 2 shows the (normalized) height of W spots calculated for various stages of growth as a function of the (normalized) distance from the center of

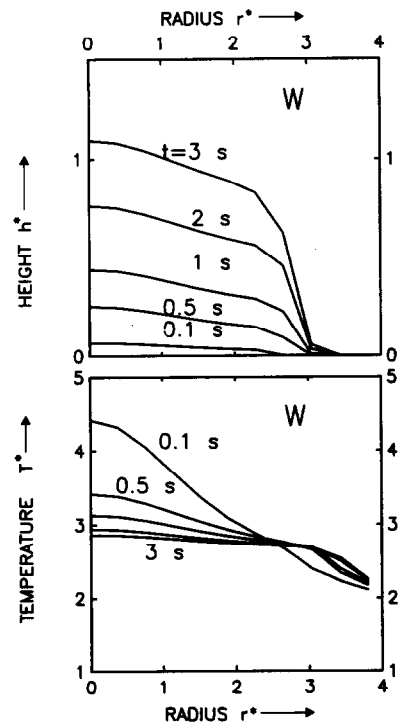

Fig. 2. Normalized height of W spots calculated for various stages of growth as a function of the (normalized) distance from the laser-beam center. The parameters employed are typical for laser-CVD of W from $WCl_6 + H_2$ (see text). The lower part of the picture shows the evolution of the (normalized) surface temperature distribution.

the laser beam. The kinetic data employed, $k_0^* = 2.14$, $\Delta E^*/T(\infty) = 5.68$, were taken from experimental investigations on the deposition of W from $WCl_6 + H_2$ [7]. The other parameters used were $T_{th}/T(\infty) = 2.71$, $\delta T_{th}/T(\infty) = 0.01$, $\kappa^*(T(\infty)) = 50.56$, $AI_0^* = 10.3$. The thermal conductivity of the deposited W is approximated by $\kappa_D(W) = c_1 + c_2/T - c_3/T^2$, where $c_1 = 42.65\ W\ m^{-1}K^{-1}$, $c_2 = 1.898 \times 10^4\ W\ m^{-1}$ and $c_3 = 1.498 \times 10^6\ W\ m^{-1}\ K$. This corresponds to one half of the heat conductivity reported in [9]. For the SiO_2 substrate we choose $\kappa_S(SiO_2) = a_1 + a_2 T$, with $a_1 = 0.9094\ W\ m^{-1}\ K^{-1}$ and $a_2 = 1.422 \times 10^{-3}\ W\ m^{-1}\ K^{-2}$ [10]. Using the Kirchhoff transforms we can approximate the relations between dimensionless quantities

$$\theta_S^*(\theta_D^*) \approx \theta_D^* + 0.46\,\theta_D^{*2}$$

and

$$T_D^* = 1 + \theta_D^* + 0.12\,\theta_D^{*2}\,.$$

The accuracy of this approximation within the temperature interval $T(\infty) = 443\ K \leq T_D \leq 2500\ K$ is 2–3%. Figure 2 demonstrates the very fast spreading in the lateral direction. The velocity of lateral growth is strongly influenced by the width of the threshold, δT_{th}. The saturation in spot diameter, which occurs when the temperature near the edge of the spot becomes smaller than the threshold temperature for deposition, is in agreement with experimental observations [7]. It becomes evident that the saturation in width takes place much faster than the saturation in height. The change in the (normalized) temperature distribution during the growth process is shown in the lower part of the figure. It shows that within a short time the surface temperature becomes almost uniform over the surface of the spot.

Figure 3 shows the growth of Ni spots deposited from $Ni(CO)_4$. In this case the thermal conductivity of the deposited Ni and of the substrate was kept constant with $\kappa^*(T(\infty) = 300\ K) = 30$. The other parameters employed in the calculations were $T(\infty) = 300\ K$, $k_0^* = 1.1 \times 10^{13}$, $\Delta E^*/T(\infty) = 45$ and $AI_0^* = 1.33$. No threshold was assumed so that $T_{th}/T(\infty) = 1$. The kinetic parameters correspond to the pyrolytic decomposition of $Ni(CO)_4$ [5]. Due to the absence of a threshold, there is no abrupt saturation in the width of Ni spots. Furthermore, the ratio of spot height to spot width is much larger than in the case of W. This is related to the much higher activation energy, ΔE^*; it yields a significantly higher growth rate in the center than near the spot edge. This behavior is in qualitative agreement with experimental observations [5, 11]. The change in temperature distribution related to the growth of the spot is similar to that observed for W.

4.2. *Direct writing of lines*

Figure 4 shows contour lines (left side) and isotherms (right side) calculated for various stages of direct writing of W lines deposited from $WCl_6 + H_2$. The

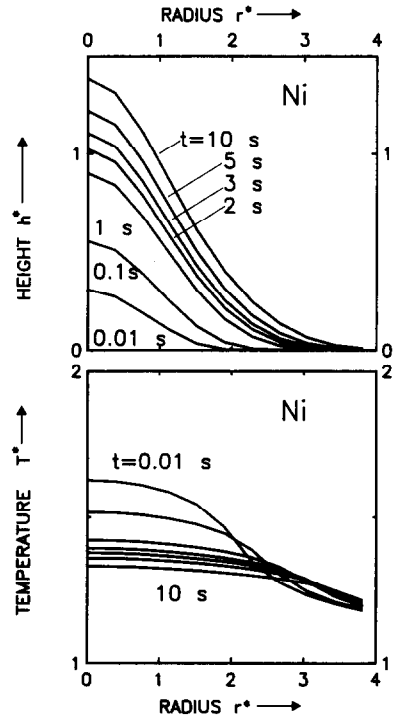

Fig. 3. Same as Fig. 2 but for Ni spots deposited from $Ni(CO)_4$.

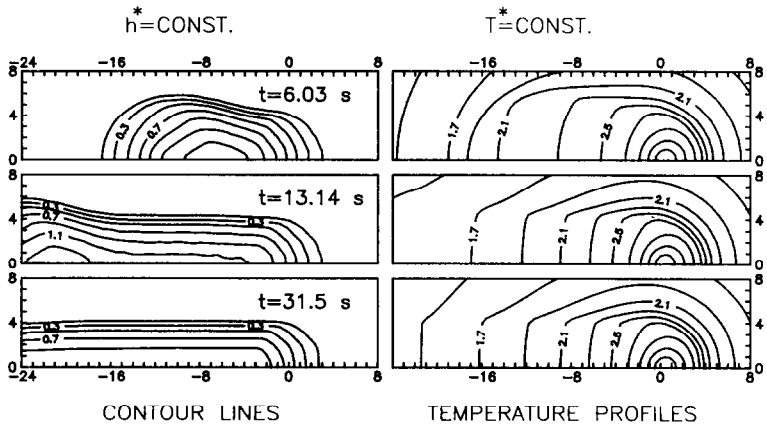

Fig. 4. Contour lines (left side) and isotherms (right side) calculated for W stripes produced by laser direct writing. The laser beam is switched on at $t = 0$.

laser beam is switched on at time $t = 0$. The scanning velocity employed was $v_S^* = 2.0$, and the absorbed laser-beam intensity $AI_0^* = 20.6$. The other parameters are the same as in Fig. 2. The figure shows that the stationary solution is achieved only after a rather long time. The larger width of the stripe observed in the initial phase of growth (short times) is related to the fact that energy

losses due to heat conduction along the stripe are not yet effective. This behavior becomes evident also from the isotherms. It is in agreement with experimental observations.

Figure 5 shows the stationary shape of a W stripe and the corresponding temperature distribution for a scanning velocity $v_S^* = 3.0$. The other parameters employed were the same as in Fig. 4. Within the regime of parameters investigated, the shape of calculated W stripes remains always uniform, i.e. it shows no oscillations in height or width [5, 12].

Calculations of the kind presented in Figs. 4 and 5 permit to derive the parameter $\xi = r_D/a$ for different scanning velocities (see also [6]). Here, a is the distance between the center of the laser beam and the tip of the stripe. From these calculations we find $1.2 < \xi < 1.5$. This value is consistent with the experimental results reported in [6].

Figure 6 shows the height (indicated by $+$), the width ($\times$), and the center temperature ($*$) calculated as a function of scanning velocity, v_S. For comparison, the corresponding dependences obtained from the one-dimensional model [6] have been included by full, dashed, and dash-dotted curves. The parameters employed were $w_0 = 7.5\ \mu m$, $\kappa_S(T(\infty)) = 0.0154\ W\ cm^{-1}\ K^{-1}$, $AI_0^* = 20.6$ ($P = 0.6$ W, $A = 0.55$). The other parameters were the same as in Figs. 2, 5 and 6. For the one-dimensional model we used $\kappa_S(1600\ K) =$

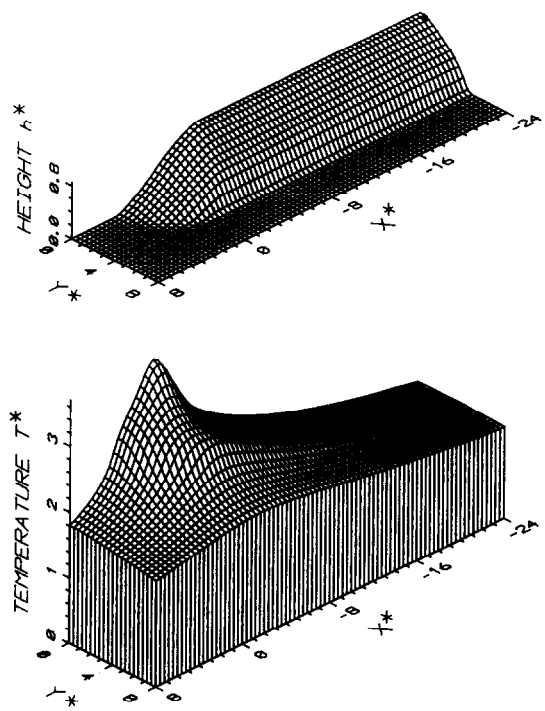

Fig. 5. Stationary profile of the (normalized) height of a W stripe and the corresponding temperature distribution.

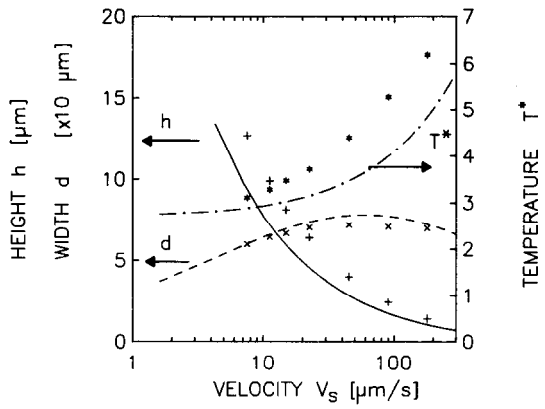

Fig. 6. Dependence of the height (+), width (×) and (normalized) center temperature (*) on scanning velocity as calculated from the two-dimensional model. For comparison, the corresponding dependences obtained from the one-dimensional model [6] have been included by full, dashed, and dash-dotted curves.

$0.032\ \mathrm{W\,cm^{-1}\,K^{-1}}$, $k_0 = 16.05\ \mu\mathrm{m/s}$, $\kappa^* = 17$, $\eta = 1.6$, $\gamma = 1.3$, $\xi = 1.25$, and $\zeta = 4/3$ (see [6]). The discrepancy between the two models is about 30%.

5. Conclusion

Two-dimensional model calculations for pyrolytic laser-CVD permit to simulate both the growth of spots and laser direct writing. The shapes of deposits calculated for different systems are in semi-quantitative agreement with those observed experimentally.

Acknowledgement

We wish to thank the "Fonds zur Förderung der wissenschaftlichen Forschung in Österreich" for financial support.

References

[1] D. Bäuerle, B. Luk'yanchuk and K. Piglmayer, *Appl. Phys. A* **50** (1990) 385.
[2] N. Kirichenko, K. Piglmayer and D. Bäuerle, *Appl. Phys. A* **51** (1990) 498.
[3] B. Luk'yanchuk, K. Piglmayer, N. Kirichenko and D. Bäuerle, *Physica A* **180** (1992) 285.
[4] N. Kirichenko and D. Bäuerle, *Thin Solid Films* **218** (1992) 1.
[5] D. Bäuerle, *Chemical Processing with Lasers*, Springer Series in Materials Science, Vol. 1, Springer, Berlin, 1986.
[6] N. Arnold, R. Kullmer and D. Bäuerle, *Microelectron. Eng.* **20** (1993) 31.
[7] R. Kullmer, P. Kargl and D. Bäuerle, *Thin Solid Films* **218** (1992) 122.

[8] W. Kräuter, D. Bäuerle and F. Fimberger, *Appl. Phys. A* **31** (1983) 13.
[9] R.C. Weast (ed.), *Handbook of Chemistry and Physics*, CRC Press, Boca Raton, FL, 59th edn., 1978/79.
[10] Data sheet Q-A 1/112, Heraeus Inc., Germany, 1979.
[11] K. Piglmayer and D. Bäuerle, in: D. Bäuerle, K.L. Kompa and L.D. Laude (eds.), *Laser Processing and Diagnostics II*, Les Editions de Physique, Les Ulis, 1986, p. 79.
[12] B. Kargl, R. Kullmer and D. Bäuerle, *Appl. Phys. A* (1993).